Extended Abstracts of the 2011 International Conference on Solid State Devices and Materials, Nagoya, 2011, pp696-697

Analyzing diffusion-like interfacial carrier transport process in pentacene organic field-effect transistors by time-resolved second harmonic generation and impendence spectroscopy

Le Zhang, Dai Taguchi, Hiroshi Masada, Takaaki Manaka, Mitsumasa Iwamoto

Department of Physical Electronics, Tokyo Institute of Technology
2-12-1 O-okayama, Meguro-ku, Tokyo 152-8552, Japan
Phone: +81-3-5734-2191 E-mail: iwamoto@ pe.titech.ac.jp

1. Introduction

During the last two decades, organic electronic devices have undergone great improvements both in materials and processing techniques [1]. Meanwhile, a number of theoretical models have also been proposed to analyze the carrier behaviour in those devices [2]. As to experimental tools, transient approaches are supposed to offer more information about the carrier behaviour inside the device, such as time of flight (TOF) [3], impedance spectroscopy (IS) [4] and transient current [5]. However, due to the ambiguities in the energetic structures of organic materials, the disorder property [3], traps [6] and contact resistance [7], the detailed understanding about the carrier behaviour in organic field-effect transistors (OFETs) are still in dispute. To solve this problem, direct probing of the carrier behaviour in OFETs is expected. Recently, we have been developing a time-resolved microscopic second harmonic generation (TRM-SHG) technique [8], which can directly probe the carrier behaviour by recording the evolution of the second harmonic (SH) intensity generated from the active layer of operating OFETs. We have applied this technique for several interesting issues [9-11].

In the present paper, diffusion-like carrier transport along the channel of a pentacene OFET was studied by using both TR-SHG and IS. In TR-SHG, the transport process of injected carriers was directly probed. On the other hand, in IS, the capacitance variations were observed. The agreements between temporal and frequency domain approaches indicate that the carrier transport along the channel follows a diffusion-like transport model driven by an interfacial charging model [11].

2. Experiment

Samples used in experiments were top-contact FET structures. Heavily doped Si wafers covered with a 500 nm thick oxide (SiO_2) layer were used as the base substrate. The material for the organic semiconductor layer was pentacene. On the surface of the substrate, a 100 nm thick PMMA was spin coated. Then, the 100 nm thick pentacene layer was evaporated onto the surface of the PMMA layer under a pressure below 10^{-6} Torr with a speed around 1 Å/s. Last, top-Au (source and drain electrodes) with a thickness of 100 nm were deposited onto the surface of the pentacene layer. Both the pentacene active layer and Au electrodes were evaporated with designed masks to reduce the edge effect. The channel width (W) of devices was same as 3 mm, but the channel lengths (L) were varied from 30, 40, 50, 60, 80 to 100 μm. The area of electrodes was estimated about 0.93 mm^2.

The arrangement of TR-SHG was the same as in our previous paper [8]. On the other hand, IS was performed by using a Solartron Impedance Spectrometer with an ac amplitude as small as 10 mV to guarantee a linear response. All measurements were carried out under ambient atmosphere.

3. Results and discussion

Figure 1(a) and (b) show the TR-SHG results of the device with a channel length of 60 μm under the electron ($V_{GS} > 0$ V) and hole ($V_{GS} < 0$ V) injection conditions, respectively.

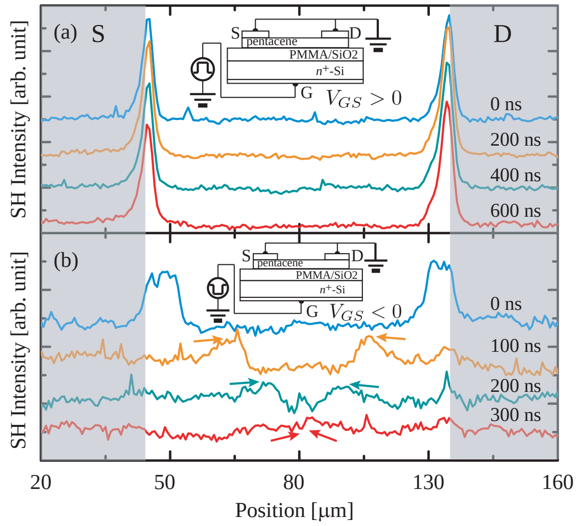

Figure 1 TR-SHG results of the device with various delay times under (a) electron (V_{GS} = 100 V) and (b) hole (V_{GS} = -100 V) injection cases, respectively. The insets show the electrical circuits.

During experiments, the source and drain electrodes were grounded and pulse voltages were applied to the gate electrode as shown in the sets of Fig. 1. The carrier behaviour under the electron injection case was shown in Fig. 1(a) under various delay times. In Fig. 1(a), there were sharp peaks near the source and drain electrodes, implying enhanced local electric fields along the channel length direction near the electrode edges. However, those peaks did not move with time but were still within the experimental time scale (~ 1 μs). Thus, it is suggested that the injected electrons accumulated just beneath the top electrodes and located at the interface between the pentacene and PMMA layers [9], resulting in a drop of the local electric field near the edges. In addition, the accumulated charges never travel along the channel, leading to a time independent SH peaks near the electrode edges. On the other hand, the TR-SHG results of the same device were totally different under the hole injection case as shown in Fig. 1(b). In Fig. 1(b), the peaks originally located at the edges of the source and drain electrodes moved along the channel with time, but with much wider peaks than that in Fig. 1(a). In addition, the height of the peaks also decreased during the movements. At about 300 ns, the two facing peaks met and merged. Because the potential difference between the two top electrodes was zero, the driving force for the carrier transport should be attributed to an interface charging model due to the accumulated charges at the interface between the pentacene and PMMA layers [11].

Figure 2(a) and (b) show the IS results with different channel lengths under the electron and hole injection cases, respectively. On the basis of TR-SHG experiments, it is proposed that the capacitance of the device under the same electrical connection shown in the sets of Fig. 1 should increase if there is diffusion-like carrier transport along the channel, which will be further enhanced for those devices with longer channel length. On the contrary, it should remain constant and independent on the channel length if the injected carriers are strongly localized. Those assumptions are well supported by the IS results shown in Fig. 2. Under the electron injection case (Fig. 2(a)), the capacitance remained constant and independent on the channel length. Nevertheless, it increased at lower frequency region and further increased with longer channel length under hole injection case (Fig 2(b)).

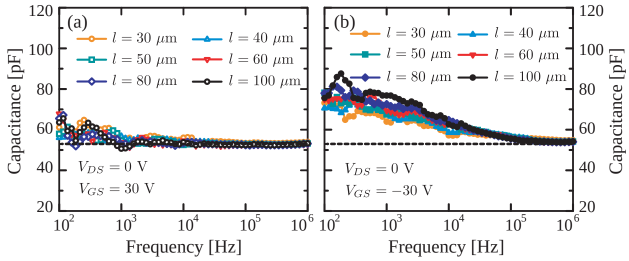

Figure 2 The IS results of OFETs with different channel lengths under (a) electron and (b) hole injection cases, respectively. The dashed lines show the geometric capacitance.

On the basis of the interface charging model, the carrier motion along the channel is related to the applied voltage V_{GS} through the Maxwell stress [11]. Since the driving force V_{GS} (100 V) in TR-SHG is 10^4 times larger than that in IS (10 mV), the transit time is supposed to be four order smaller in TR-SHG [4]. In TR-SHG, the transit time was estimated as 0.3 μs, while the saturation frequency f_{sat} in Fig. 2(b) corresponded to a transit time about 3 ms (=1/f_{sat}, f_{sat} ~0.34 kHz). It should be noted that although the detailed analysis at lower frequency was difficult due to the experimental limits, the agreements between two experiments were acceptable.

The channel length dependent capacitance under both hole and electron injection cases was shown in Fig. 3. The capacitance exhibits no channel length dependence under the electron injection case. However, it increased linearly with channel length under the hole injection case.

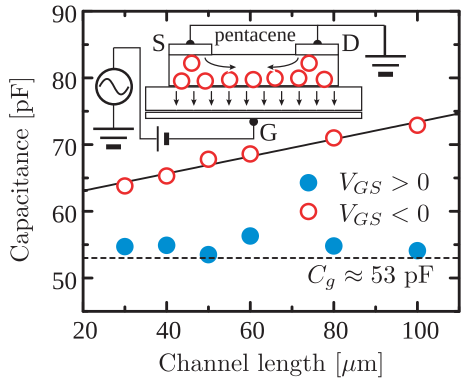

Figure 3 Channel length dependent capacitance under electron (V_{DC} = 30 V) and hole (V_{DC} = -30 V) injection cases. The inset shows the proposed model. The measured frequency is 2 kHz. C_g is the geometric capacitance.

4. Conclusions

We had demonstrated the diffusion-like carrier transport process along the channel of OFETs by using both TR-SHG and IS. In TR-SHG, the transport process was revealed under the hole injection case. Correspondingly, in IS, the capacitance increased at the lower frequency region when holes were injected. Furthermore, the capacitance showed a channel length dependence under the hole injection case, which further supported the diffusion-like model. It is proposed that the interface charging was the driving force for the diffusion-like transport.

Acknowledgements

A part of this work is financially supported by a Grant-in-Aid for scientific research (S) (Grant No. 22226007) and a Grant-in-Aid for Young Scientists (B) (No.22760227).

References

[1] H. Klauk, Chem. Soc. Rev. **39**, 2643 (2010).
[2] H. Bässler, Phys. Status Solidi B **175**, 15 (1993).
[3] M. Weis, J. Lin, D. Taguchi, T. Manaka, and M. Iwamoto, J. Phys. Chem. C. **113**, 18459 (2009).
[4] L. Zhang, D. Taguchi, J. Li, T. Manaka, and M. Iwamoto, Appl. Phys. Lett. **98**, 092109 (2011).
[5] X. Y. Chen, H. Zhu, and S. D. Wang, Appl. Phys. Lett. **97**, 243301 (2011).
[6] T. Manaka, F. Liu, M. Weis, and M. Iwamoto, J. Appl. Phys. **107**, 043712 (2010).
[7] M. Weis, J. Lin, D. Taguchi, T. Manaka, and M. Iwamoto, Appl. Phys. Lett. **97**, 263304 (2011).
[8] T. Manaka, E. Lim, R. Tamura, and M. Iwamoto, Nat. Photonics **1**, 581 (2007).
[9] L. Zhang, D. Taguchi, J. Li, T. Manaka, and M. Iwamoto, J. Appl. Phys. **108**, 093707 (2010).
[10] D. Taguchi, D. M. Weis, T. Manaka, and M. Iwamoto, Appl. Phys. Lett. **95**, 263310 (2009).
[11] M. Weis, J. Lin, D. Taguchi, T. Manaka, and M. Iwamoto, Jpn. J. Appl. Phys. **49**, 071603 (2010).